

INVESTIGATION OF BILAYER $\text{YBa}_2\text{Cu}_3\text{O}_{7-x}\text{-Ca}_3\text{Co}_4\text{O}_9$ THERMOELECTRIC CERAMIC PREPARED BY SOLID-STATE SINTERING METHOD

Pimpilai Wannasut^{a,b}, Pilin Eaksuwanchai^c, Anucha Watcharapasorn^{a, d,*}

^aDepartment of Physics and Materials Science, Faculty of Science, Chiang Mai University, Chiang Mai, 50200, Thailand

^bGraduate School, Chiang Mai University, Chiang Mai, 50200, Thailand

^cGraduate School of Engineering, Osaka University, 2-1 Yamadaoka, Suita, Osaka, 565-0871, Japan

^dMaterials Science Research Center, Faculty of Science, Chiang Mai University, Chiang Mai, 50200, Thailand

Received 27 December 2016; Revised 31 March 2017; Accepted 6 April 2017

ABSTRACT

Recently, segmented thermoelectric materials have been undeniably popular owing to their highly efficient heat-to-electricity conversion capability. This work therefore focuses on the preparation of bilayer thermoelectric $\text{YBa}_2\text{Cu}_3\text{O}_{7-x}\text{-Ca}_3\text{Co}_4\text{O}_9$ or YBCO-CCO ceramics by solid-state reaction and sintering method. YBCO calcined at 850°C for 12 h showed pure phase with orthorhombic structure and $\text{Ca}_3\text{Co}_4\text{O}_9$ calcined at 750°C for 24 h showed pure phase with hexagonal structure. The optimum condition for sintering the YBCO-CCO ceramic included 900°C sintering temperature and 18 h holding time under a normal atmosphere. This sintering condition was also applicable to all YBCO-CCO samples regardless of the layer thickness. Good bonding of the cylindrical-shaped bilayer YBCO-CCO ceramics seemed to be caused by interfacial reaction between two compounds. Based on the high values of the power factor of individual YBCO and CCO layers, it was expected that the bilayer YBCO-CCO ceramic would give enhanced power factor similar to those of state-of-the-art segmented thermoelectrics.

KEYWORDS: Segmented thermoelectric; Bilayer YBCO-CCO; Solid-state sintering method

*

Corresponding authors; e-mail: anucha@stanfordalumni.org, Tel: +66-5394-3367

INTRODUCTION

As the world keeps using natural resources for daily human activities and industrial manufacturing, as much as 70% of input energy is lost to the environment [1]. The renewable and environmentally “green” source of energy has been required. A type of alternative energy devices that can directly converted thermal energy to electricity is now made of intermetallic, semiconducting or oxide thermoelectric (TE) materials. In these TE materials, electron and hole diffusion are driven by temperature drop between the hot- and cold-ends and the potential difference between the two ends occurred. This phenomenon determines the Seebeck coefficient, which is one of the most important parameters in thermoelectric properties [2]. The overall performance of TE materials is generally evaluated by the dimensionless figure of merit equation:

$$ZT = S^2\sigma T/\kappa$$

where Z is the figure of merit, T absolute temperature, S Seebeck coefficient, σ electrical conductivity and κ total thermal conductivity [3]. Certain TE materials, particularly Bi-Te-based alloys, have already been used in various devices such as electricity generators, TE modules and cooler/heater [4–7]. To optimize thermoelectric properties over a wider range of temperature, segmented thermoelectric unicouples were initially investigated by the Jet Propulsion Laboratory (JPL). Caillat *et al.* studied segmented of novel p-type Zn_4Sb_3 , p-type $\text{CeFe}_4\text{Sb}_{12}$ -based alloys and n-type CoSb_3 -based alloys and found an increase in thermoelectric efficiency by about 15% [8]. Recently, Le *et al.* [9] studied a segmented thermoelectric oxide between p-HH/ $\text{Ca}_3\text{Co}_4\text{O}_9$

and $n\text{-Zn}_{0.98}\text{Al}_{0.02}\text{O}$ which showed improved thermoelectric performance with ~5% conversion efficiency.

Therefore, this work attempted to prepare a bilayer of $\text{YBa}_2\text{Cu}_3\text{O}_{7-x}$ (YBCO) - $\text{Ca}_3\text{Co}_4\text{O}_9$ (CCO) ceramic via the solid-state sintering method. YBCO is a well-known high- T_c superconductor and at its stoichiometric composition, the compound had exceptionally high electrical conductivity value ($50,000 \Omega^{-1}\text{m}^{-1}$ at 300 K) [10–11]. However, in terms of Seebeck coefficient, the value was very low ($S < 10 \mu\text{V/K}$) [12]. On the other hand, Prayoonphokkharat *et al.* [13] reported that $\text{YBa}_2\text{Cu}_3\text{O}_{7-x}$ ceramic possessed high value of ZT (~2) due to its high electrical conductivity ($50,000 \Omega^{-1}\text{m}^{-1}$) at a temperature slightly higher than room temperature coupled with moderately high Seebeck coefficient (~500 $\mu\text{V/K}$) and low thermal conductivity (~1.6 W/mK). For CCO, this material is known to have a misfit layered structure with potentially high ZT value (~0.87) at high temperature [14]. Prasertsopa *et al.* [15] similarly reported electrical conductivity of $4,000 \Omega^{-1}\text{m}^{-1}$ and moderate Seebeck coefficient (170 $\mu\text{V/K}$).

By forming the YBCO-CCO bilayer ceramic whose optimum ZT values could be obtained at low and high temperature, respectively, thermoelectric properties are expected to be enhanced. Microstructural, chemical and electrical property measurements are therefore carried out and discussed in this work.

MATERIALS AND METHODS

Starting materials for preparation of the $\text{YBa}_2\text{Cu}_3\text{O}_{7-x}$ (YBCO) and $\text{Ca}_3\text{Co}_4\text{O}_9$ (CCO) powders in this study were Y_2O_3 (99.99%, Aldrich), BaCO_3 ($\geq 99\%$, Sigma-Aldrich), CuO (98%, Sigma-Aldrich), CaCO_3 (99.5%, Aldrich) and Co_3O_4 (99.5%, Aldrich). The moisture in BaCO_3 and CaCO_3 powders was removed by heating in an oven for 24 hrs. The weighted powders were mixed by using wet ball milling in 99.9% ethanol for 24 hrs and dried in an oven at 120°C for 24 hrs. YBCO powder was calcined at 850°C for 12 hrs and CCO powder was calcined at 750°C for 24 hrs in a normal atmosphere with heating and cooling rate of $5^\circ\text{C}/\text{min}$. The green compacts of YBCO, CCO and bilayer YBCO-CCO were formed using a uniaxial pressing technique (see Figure 1).

The YBCO and CCO green pellets were sintered at $900\text{--}1050^\circ\text{C}$ for 12 hrs and $950\text{--}1050^\circ\text{C}$ for 24 hrs, respectively. The bilayer was sintered at a temperature of 900°C for 18 hrs. The heating and cooling rates for the sintering process were $5^\circ\text{C}/\text{min}$. X-ray diffractometer (XRD, Lab X-

6000) was used for analyzing the phases of powder and ceramics. The microstructure was determined by scanning electron microscopy (SEM, JEOL JSM-6335F). The power factor of individual YBCO and CCO ceramics was investigated using a Seebeck coefficient/Electrical resistant measurement system (ZEM-3, Ulvac).

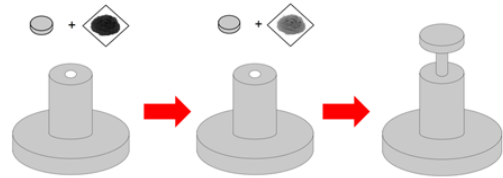


Fig. 1 YBCO-CCO bilayer preparation by uniaxial pressing.

RESULTS AND DISCUSSION

Figure 2(a) and 2(b) show XRD pattern of calcined YBCO and CCO powders, respectively. The patterns presented single phase and no secondary phase was observed. This indicated that starting materials reacted completely during calcination process.

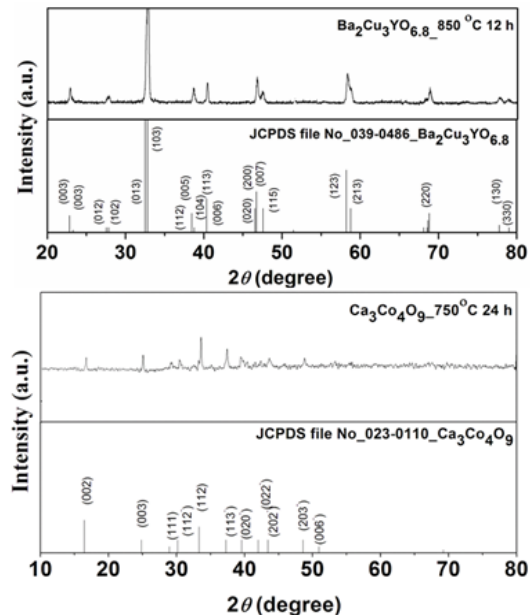


Fig. 2 XRD patterns of (a) YBCO powder and (b) CCO powder.

Figure 3 shows the density of YBCO and CCO ceramics. The optimum values of 5.47 g/cm^3 at the sintering temperature of 950°C for 12 hrs and 5.72 g/cm^3 at 1000°C for 24 hrs were obtained for YBCO and CCO, respectively. The resulting YBCO and CCO ceramics presented regular

shape, undistorted and not melting. It was believed that an increase in the sintering temperature caused a driving force for mass transfer to increase. This led to an enhancement of the sintering capability of the ceramics. However, as the sintering temperature increased further, the density of the ceramics was then dropped. This was attributed to an evaporation of a raw component and a re-emergence of pores, leading to a decrease of a density of the ceramics [16]. By varying the sintering condition, i.e. from 900–1000°C and 12–20 hrs, for preparing the bilayer YBCO-CCO ceramic, the most suitable sintering temperature was found to be 900°C and 18 hrs holding time. The interfacial bonding between YBCO and CCO showed no distortion and cracks as observed by an SEM backscattered image shown in Figure 4.

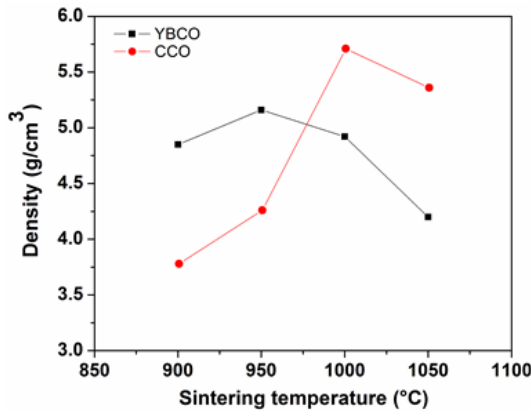


Fig. 3 Plot of the density YBCO and CCO as a function of temperature.

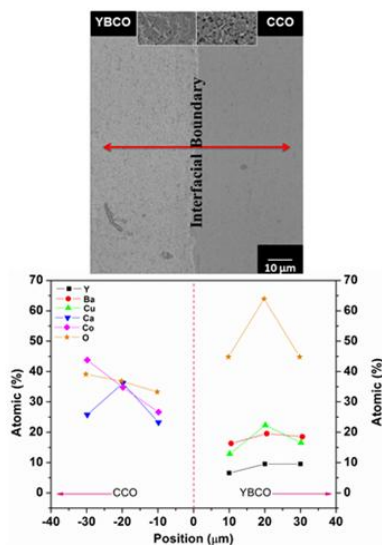


Fig. 4 Backscattered electron image and compositional variation of bilayer YBCO-CCO ceramic.

YBCO showed light color while CCO indicated dark color owing to their difference in apparent atomic mass and hence electron scattering capability [17].

XRD patterns of YBCO-side and CCO-side of the bilayer corresponded to the standard file No. 39-0486 of $\text{YBa}_2\text{Cu}_3\text{O}_{7-x}$ in the orthorhombic space group (Figure 5(a)) and file No. 023-011 of $\text{Ca}_3\text{Co}_4\text{O}_9$ as a monoclinic structure (Figure 5(b)), respectively. Energy dispersive X-ray spectrometry (EDS) near the interfacial boundary of the bilayer showed elemental composition corresponding to CCO and YBCO layer. There was some compositional variation of each element at various positions away from the interface. This could be due to some diffusion/reaction that may occur at the interface. However, the extent and exact compositional difference on each side may have to be investigated more precisely. Overall, the chemical composition of each side at the distance greater than 30 μm from the interface should belong to that of CCO and YBCO layers.

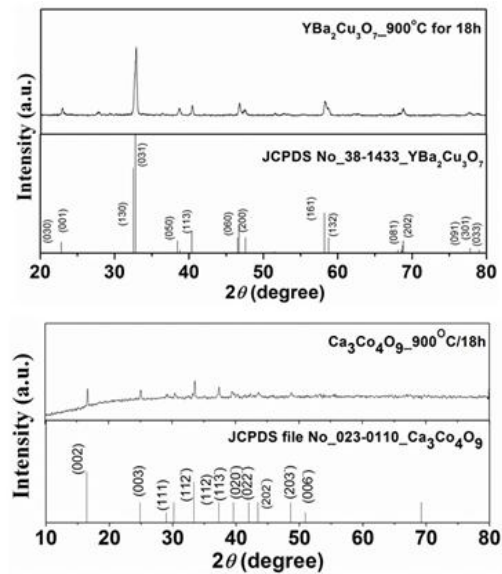


Fig. 5 XRD patterns of (a) YBCO-side and (b) CCO-side of bilayer YBCO-CCO ceramic.

Figure 6 shows the plot of electrical conductivity and Seebeck coefficient as a function of temperature of YBCO and CCO ceramics measured from 373–973 K. Electrical conductivity of all samples decreased with increasing temperature which indicated the metallic conduction behavior in which the mobile charge carriers were scattered more strongly at high temperature. YBCO showed high electrical conductivity of $88,000 \Omega^{-1}\text{m}^{-1}$ while CCO showed the value of $60,000 \Omega^{-1}\text{m}^{-1}$ at temperature of 373

K. The value of CCO at high temperature (~973 K) was also in agreement with that reported by Zhang *et al.* [18]. The temperature dependence of Seebeck coefficient (S) of YBCO and CCO ceramics measured at 373–973 K shows an increasing trend with increasing temperature. This also indicated the metallic-like conduction of both compounds [4–6]. The S values of all samples showed positive value which implied that holes were the major carriers and the compounds had a p-type conduction.

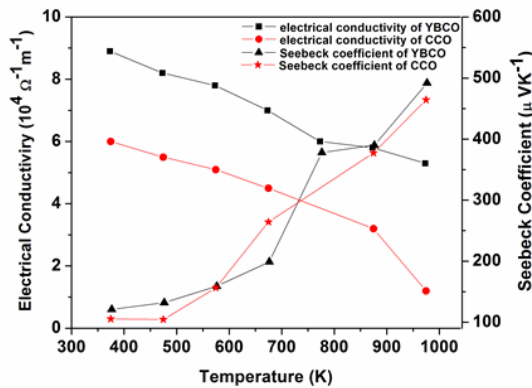


Fig. 6 Electrical conductivity and Seebeck coefficient of YBCO and CCO ceramics.

The calculated power factor values of all samples are shown in Figure 7. The power factor of YBCO and CCO samples showed an increasing trend with increasing temperature and their values ranged from 0.3–0.8 $\mu W/mK^2$. These values are relatively high compared to some of the state-of-the-art compounds such as Na_xCoO_2 and $Ag_{0.86}Pb_{22}SbTe_{20}$ [19]. Thus, It is expected that the bilayer YBCO-CCO would provide enhanced thermoelectric conversion efficiency and could be used as a potential p-type leg in a unicycle module.

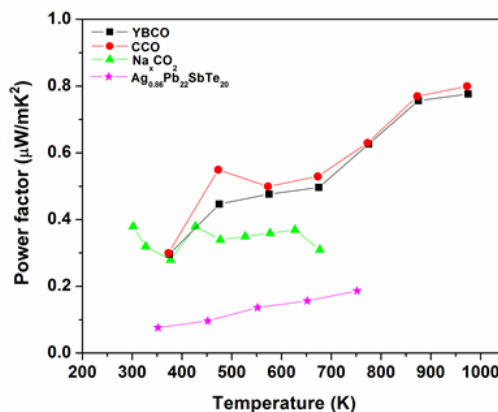


Fig. 7 Power factor of YBCO and CCO ceramics.

CONCLUSION

This work successfully prepared the bilayer of YBCO-CCO thermoelectric ceramics via a solid-state sintering method. The suitable condition for sintering temperature was 900°C for 18 hrs. The bilayer had no observed secondary phases on each side. The interface of the bilayer showed a distinct boundary between YBCO and CCO but with some compositional variations of elements across the region. The power factor of YBCO and CCO ceramics showed relatively high values at a wide range of temperature which indicated that the bilayer of these compounds should provide better thermoelectric conversion efficiency than individual compounds and may be considered as a p-type thermoelectric leg.

ACKNOWLEDGEMENTS

This research was financially supported by the Thailand Research Fund (TRF-RSA5880005 and IRG5780013) and Thailand Institute of Scientific and Technological Research. Partial supports from the Center of Excellence in Materials Science and Materials Technology, the National Research University Project under Thailand's Office of the Higher Education, Faculty of Science, and the Graduate School, Chiang Mai University are also acknowledged. P. Wannasut would also like to thank the financial support from the TRF through the Royal Golden Jubilee Ph.D Program (PhD 0173/2558).

REFERENCES

- [1] Thinkgeek, <http://www.thinkgeek.com>, 10 December 2016
- [2] T. Ming, Y. Wu, C. Peng, Y. Tao, Thermal analysis on a segmented thermoelectric generator, *Energy*. 80 (2015) 388–399.
- [3] X. Tang, T. M. Tritt, Overview of thermoelectric sodium cobaltite: Na_xCoO_4 , *J. S. C. Acad. Sci.* 6(2) (2008) 10–13.
- [4] K. Kurosaki, H. Muta, M. Uno, S. Yamanaka, Thermoelectric properties of $NaCo_2O_4$, *J. Alloy Compd.* 315 (2001) 234–236.
- [5] M. Ito, D. Furumoto, Effects of noble metal addition on microstructure and thermoelectric properties of Na_xCoO_4 , *J. Alloy. Compd.* 450 (2008) 494–498.
- [6] L. Wang, M. Wang, D. Zhao, Thermoelectric properties of c-axis oriented Ni-substituted $NaCoO_2$ thermoelectric oxide by the citric acid complex method, *J. Alloy. Compd.* 471 (2009) 519–523.
- [7] M. Presecnik, J. de Boer, S. Bernik, Synthesis of

- single-phase $\text{Ca}_3\text{Co}_4\text{O}_9$ ceramics and their processing for a microstructure-enhanced thermoelectric performance, *Ceram. Int.* 42 (2016) 7315–7327.
- [8] T. Caillat, J.P. Fleurial, J. Snyder, A. Zoltan, D. Zoltan, A. Borshchevsky, A new high efficiency segmented thermoelectric, 34th Intersociety Energy Conversion Engineering Conference, Vancouver British Columbia. 2–5 August 1999, 2567.
- [9] T. H. Le, N. Pryds, N. Van Nong, S. Linderoth, Segmented thermoelectric oxide-based module, Department of Energy Conversion and Storage, Technical University of Denmark, 2014.
- [10] X. Wei, R. S. Nagarajan, E. Peng, J. Xue, J. Wang, J. Ding, Fabrication of $\text{YBa}_2\text{Cu}_3\text{O}_{7-x}$ (YBCO) superconductor bulk structures by extrusion freeforming, *Ceram Int.* 42 (2016) 15836–15842.
- [11] N. V. Tri, Modulated Structure and Superconducting Nano-Micromechanism in YBCO Compounds, *Ferroelectrics.* 305 (2004) 141–145.
- [12] J.E. Rodriguez, J. Lopez, Thermoelectric figure of merit of oxygen-deficient YBCO perovskites, *Physica B.* 387 (2007) 143–146.
- [13] P. Prayoonphokkharat, S. Jiansirisomboon, A. Watcharapasorn, Fabrication and properties of $\text{YBa}_2\text{Cu}_3\text{O}_{7-x}$ ceramics at different sintering temperatures, *Electron Mater Lett.* 9 (4) (2013) 413–416.
- [14] D. Wang, L. Chen, Q. Yao, J. Li, High-temperature thermoelectric properties of $\text{Ca}_3\text{Co}_4\text{O}_{9+\delta}$ with Eu substitution, *Solid. State. Commun.* 129 (2004) 615–618.
- [15] N. Prasetsopha, S. Pinitsoontorn, V. Amornkitbamrung, High Temperature Thermoelectric and optical properties of $\text{Ca}_3\text{Co}_4\text{O}_9$ prepared by thermal hydrodecomposition, *Chiang Mai J. Sci.* 40(6) (2013) 1030-1034.
- [16] B. Fang, N. Jiang, C. Ding, Q. Du, J. Ding, Decrease of sintering temperature by CuO doping of the $0.8\text{Pb}(\text{Mg}_{1/3}\text{Nb}_{2/3})\text{O}_3-0.2\text{PbTiO}_3$ ceramics prepared by reaction-sintering method, *Phys. Status Solidi A.* 209 (2012) 254–261.
- [17] W. D. Callister, Materials science and engineering an introduction, 6th Edition, John Wiley & Sons Ltd. New York, 2003.
- [18] Y. Zhang, J. Zhang, Q. Lu, Synthesis of highly textured $\text{Ca}_3\text{Co}_4\text{O}_9$ ceramics by spark plasma sintering, *Ceram. Inter.* 33 (2007) 1305–1308.
- [19] M. Zhou, J.F. Li, T. Kita, Nanostructured $\text{AgPb}_m\text{SbTe}_{m+2}$ System Bulk Materials with Enhanced Thermoelectric Performance, *J. Am. Chem. Soc.* 130 (2008) 4527–4532.